Operation of a Continuously Frequency-Tunable Second-Harmonic CW 330-GHz Gyrotron for Dynamic Nuclear Polarization

Antonio C. Torrezan, *Member, IEEE*, Michael A. Shapiro, Jagadishwar R. Sirigiri, *Member, IEEE*, Richard J. Temkin, *Fellow, IEEE*, and Robert G. Griffin

***Abstract*—The design and the operation of a frequency-tunable continuous-wave (CW) 330-GHz gyrotron oscillator operating at the second harmonic of the electron cyclotron frequency are reported. The gyrotron has generated 18 W of power from a 10.1-kV 190-mA electron beam working in a $TE_{-4,3}$ cylindrical mode, corresponding to an efficiency of 0.9%. The measured start oscillation current over a range of magnetic field values is in good agreement with theoretical start currents obtained from linear theory for successive high-order axial modes $TE_{-4,3,q}$, where $q = 1$–6. Moreover, the observed frequency range in the start current measurement is in reasonable agreement with the frequency range obtained from numerical simulations. The minimum start current was measured to be 33 mA. A continuous tuning range of 1.2 GHz was experimentally observed via a combination of magnetic, voltage, and thermal tuning. The gyrotron output power and frequency stabilities were assessed to be $\pm 0.4\%$ and ± 3 ppm, respectively, during a 110-h uninterrupted CW run. Evaluation of the gyrotron output microwave beam pattern using a pyroelectric camera indicated a Gaussian-like mode content of 92% with an ellipticity of 28%. The gyrotron will be used for 500-MHz nuclear magnetic resonance experiments with sensitivity enhanced by dynamic nuclear polarization.**

***Index Terms*—Dynamic nuclear polarization (DNP), nuclear magnetic resonance (NMR), second cyclotron harmonic, submillimeter wave, terahertz, tunable gyrotron.**

I. Introduction

GYROTRON oscillators are vacuum electron devices that have delivered megawatt power levels at millimeter wavelengths [1] and kilowatt power levels in the terahertz or submillimeter band [2], [3]. The lack of other sources that are able to match these power levels in the aforementioned bands, with the exception of much bulkier free-electron lasers, makes the gyrotron the oscillator of choice in many applications such as plasma heating [1], materials processing [4], diagnostics [5], spectroscopy [6], and in nonlethal weapons [7]. Although the main attractiveness of the gyrotron resides in its power, some applications would also benefit from having a frequency-tunable generator. For instance, the operation of a nuclear magnetic resonance (NMR) spectrometer enhanced by dynamic nuclear polarization (DNP) would be greatly simplified by utilizing a continuously tunable continuous-wave (CW) gyrotron [8].

For efficient interaction between electrons and electromagnetic waves, gyrotron oscillators employ resonant structures with high quality factor, on the order of or greater than 1000, depending on the operating frequency. This limits the attainable frequency tunability of a given gyrotron cavity mode to the linewidth associated with its quality factor [9]. Another option for broader tunability is to excite successive cavity modes with eigenfrequencies close to each other by changing the electron cyclotron frequency by means of the gyrotron main magnetic field and/or the electron beam energy. As in gyrotron resonators the axial wavenumber is typically much smaller than the transverse wavenumber, cavity modes that only differ by their number of axial variations on their electric field profile may lead to continuous tunability. This tuning scheme was demonstrated in a millimeter-wave gyrotron operating in the first harmonic of the electron cyclotron frequency, both in pulsed mode [10] and in CW mode [11], and later in a second-harmonic CW terahertz gyrotron [12], [13]. The smooth tuning range obtained in these experiments was equal to or greater than 1 GHz. Following these results, other gyrotrons using a similar magnetic tuning scheme have been built, as described in [14], [15].

In this paper, we report the design and the operation of a second-harmonic CW 330-GHz gyrotron oscillator. Based on previous second-harmonic broadband magnetic and voltage tuning results at 332 GHz [12], [16], this tuning scheme was favored for the 330-GHz gyrotron, instead of a more involved approach using mechanical tuning [17], [18]. Besides further exploring the chosen tuning scheme, the 330-GHz gyrotron also features additional tuning by thermally expanding the resonator. The 330-GHz gyrotron is intended to be used as a terahertz source for a 500-MHz DNP/NMR spectrometer. This paper is organized as follows: The design of the gyrotron is described in

Manuscript received February 2, 2011; revised April 14, 2011; accepted April 15, 2011. Date of publication June 2, 2011; date of current version July 22, 2011. This work was supported by the U.S. National Institutes of Health under Grant EB1960, Grant EB001965, Grant EB002026, Grant EB002804, and Grant EB004866. The review of this paper was arranged by Editor W. L. Menninger.

A. C. Torrezan was with the Department of Electrical Engineering and Computer Science and the Plasma Science and Fusion Center, Massachusetts Institute of Technology, Cambridge, MA 02139 USA. He is now with the Hewlett–Packard Co., Palo Alto, CA 94304 USA.

M. A. Shapiro is with the Plasma Science and Fusion Center, Massachusetts Institute of Technology, Cambridge, MA 02139 USA.

J. R. Sirigiri was with the Plasma Science and Fusion Center, Massachusetts Institute of Technology, Cambridge, MA 02139 USA. He is now with Bridge12 Technologies Inc., Cambridge, MA 02139 USA.

R. J. Temkin is with the Department of Physics and the Plasma Science and Fusion Center, Massachusetts Institute of Technology, Cambridge, MA 02139 USA (e-mail: temkin@mit.edu).

R. G. Griffin is with the Department of Chemistry and the Francis Bitter Magnet Laboratory, Massachusetts Institute of Technology, Cambridge, MA 02139 USA.

Color versions of one or more of the figures in this paper are available online at http://ieeexplore.ieee.org.

Digital Object Identifier 10.1109/TED.2011.2148721

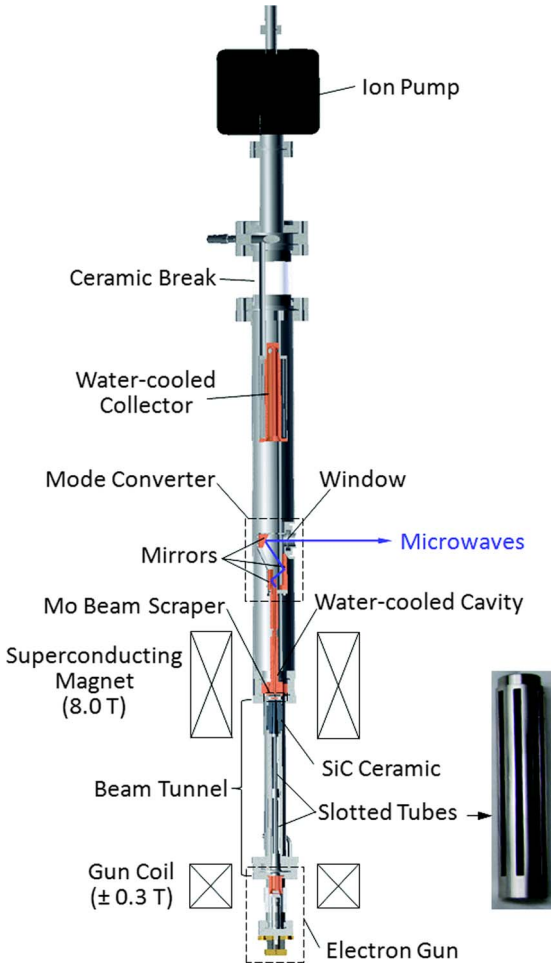

Fig. 1. Schematic of the 330-GHz gyrotron oscillator. A picture of a slotted tube utilized in the gyrotron beam tunnel is also shown.

Section II, while Section III details the experimental characterization of the device including evaluation of output power and frequency as a function of magnetic field, beam voltage, and cavity cooling temperature. Measured start oscillation current of the operating mode, frequency and power stabilities in long-run continuous operation, and output microwave beam profile are also reported in Section III. Conclusions follow in Section IV.

II. Design

The 330-GHz gyrotron oscillator is shown schematically in Fig. 1. This gyrotron employs a diode magnetron injection gun described in [13]. The electron gun is connected to a CW power supply that is able to provide a maximum voltage of 25 kV and a maximum current of 200 mA, restricted to a maximum total power of 4 kW. The beam tunnel section between the electron gun and the gyrotron resonator is composed of a series of slotted tubes and a piece of lossy SiC ceramic [19] to prevent spurious oscillations before the interaction region. The loss tangent of the employed SiC was estimated to be 0.02 at 200 GHz based on transmission measurements performed with an Agilent E8363B vector network analyzer with a 90–220-GHz extension module. The electron beam radius at the oscillator beam-wave interaction section is $r_e = 1.08$ mm. Other design

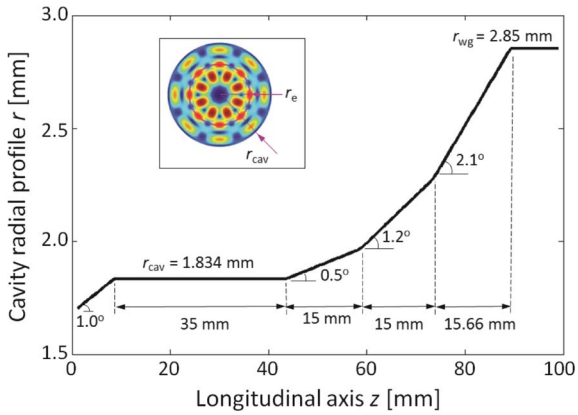

Fig. 2. Schematic of the 330-GHz gyrotron interaction circuit. The inset shows the transverse electric field profile of the cavity mode $TE_{-4,3}$ and the location of the electron beam with radius $r_e = 1.08$ mm.

TABLE I
Cold-Cavity Parameters for $TE_{-4,3,q}$ Modes and Respective Frequency Band

q	f [GHz]	Q_D	Q	$f - f/Q$	$f + f/Q$
1	329.96	81500	9030	329.92	330.00
2	330.03	20400	6780	329.98	330.08
3	330.15	9050	4780	330.08	330.22
4	330.32	5080	3390	330.22	330.42
5	330.54	3230	2450	330.41	330.67
6	330.81	2230	1830	330.63	330.99
7	331.13	1670	1430	330.90	331.36

beam parameters were calculated to be pitch factor $\alpha \cong 2$ and electron perpendicular velocity spread of 4% at a beam voltage $V_b = 10.1$ kV. The pitch factor and the velocity spread were obtained using the code EGUN [20].

The high coupling coefficient of the second-harmonic cylindrical mode $TE_{-4,3}$ at the designed beam radius, along with previous experiments carried out in this mode at 332 GHz [12], [16], motivated its choice as the gyrotron operating mode. The profile of the designed oscillator interaction circuit is presented in Fig. 2, where the inset shows the position of the electron beam with respect to the transverse electric field profile of the operating cavity mode $TE_{-4,3}$. A long interaction cavity straight section was preferred in order to lower the start oscillation current and facilitate the excitation of high-order axial modes $TE_{-4,3,q}$ for frequency tunability via magnetic and voltage tuning schemes. Indexes m, p, and q associated with a cylindrical mode $TE_{m,p,q}$ correspond to the azimuthal, radial, and axial mode numbers, respectively.

The ohmic quality factor Q_O for the different axial modes $TE_{-4,3,q}$ was calculated to be $Q_O = 10150$, assuming an equivalent copper electrical conductivity of 2.9×10^7 S/m, which is half of ideal copper (5.8×10^7 S/m). The eigenfrequency f and the diffraction quality factor $Q_{D,q}$ of each axial mode were computed using a cold-cavity code [21], and the results are presented in Table I. The total quality factor Q and the frequency band for each axial mode are also shown in Table I.

From the calculated total quality factors and the cold axial electric field profile, the start oscillation current for the operating and neighboring modes were computed using the linear theory [22]. The start current for the first axial variation ($q = 1$)

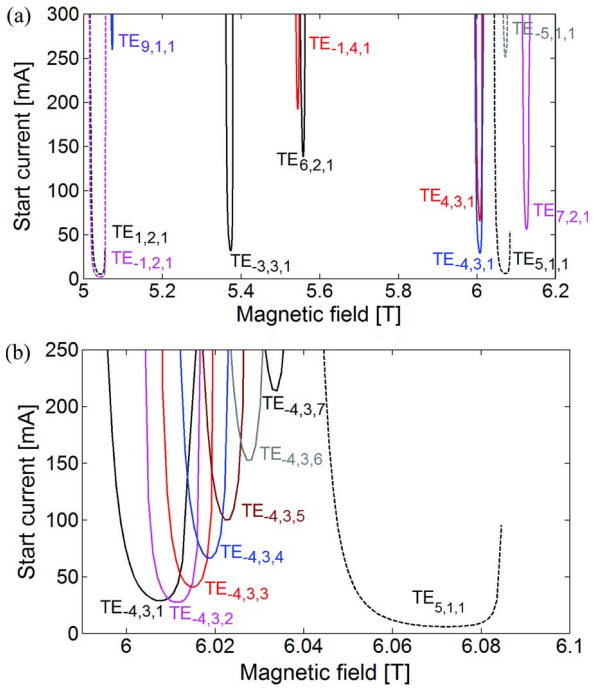

Fig. 3. (a) Calculated start oscillation current of cavity $TE_{m,p,1}$ modes adjacent to the operating mode $TE_{-4,3,1}$; (b) calculated start current of high-order axial operating modes $TE_{-4,3,q}$, where $q = 1$–7, and neighboring fundamental mode $TE_{5,1,1}$. In (a) and (b), dashed lines represent fundamental-harmonic modes, while solid lines refer to second-harmonic modes (Beam parameters: $V_b = 10.1$ kV, $r_e = 1.08$ mm, $\alpha = 1.8$, and 5% beam perpendicular velocity spread).

of each mode is shown in Fig. 3(a) for beam parameters $V_b = 10.1$ kV, $\alpha = 1.8$, $r_e = 1.08$ mm, and 5% electron perpendicular velocity spread. The minimum start current for the mode $TE_{-4,3,1}$ was computed to be 29 mA. The calculated start current for the high-order axial operating modes $TE_{-4,3,q}$ and the adjacent mode, i.e., the fundamental-harmonic mode $TE_{5,1,1}$, are displayed in Fig. 3(b) for the same beam parameters. Based on the start current calculation and the current limit of 200 mA in the available power supply, the linear theory predicts that it may be possible to excite high-order axial modes that would yield a tuning range on the order of 1 GHz in this gyrotron.

The gyrotron interaction circuit was electroformed from oxygen-free copper using a stainless steel mandrel machined to a tolerance of 2.5 μm in cavity diameter and with a surface finish of 0.2 μm. The fabricated cavity was cold tested using the aforementioned vector network analyzer and a step-cut Vlasov antenna connected to the cavity uptapered section. Lower order modes excited into the gyrotron resonator were identified as $TE_{0,1,1}$ and $TE_{1,2,1}$ based on the measured resonant frequency, which were corrected for vacuum, and the good agreement between the measured loaded quality factor and the calculated total quality factor. The calculated total quality factor also assumes a copper conductivity of 2.9×10^7 S/m and diffractive Q_D obtained from the cold-cavity code. The cold test results are summarized in Table II. Based on these results, the cavity radius was estimated to be $r_{\rm cav} = 1.834$ mm, which is within the manufacturing tolerance.

After the beam-wave interaction, the generated wave is extracted from the gyrotron oscillator by converting the cylindrical operating mode to a Gaussian-like microwave beam. The mode converter consists of a helical launcher with waveguide radius $r_{\rm wg} = 2.85$ mm, a quasi-parabolic smooth mirror, and two additional smooth mirrors. The mode converter design was evaluated using the electric-field integral equation code Surf3d [23]. The results from these calculations are shown in Fig. 4, where the output beam amplitude is 92% Gaussian with the beam waist sizes $w_x = 3.3$ mm and $w_y = 4.2$ mm at the focal plane, which is located 40 mm after the window plane.

TABLE II
COLD TEST RESULTS OF FABRICATED GYROTRON RESONATOR

Experiment			Theory
Mode	Resonant frequency [GHz]	Q	Q
$TE_{0,1,1}$	99.77	2600	2450
$TE_{1,2,1}$	138.78	4370	3980

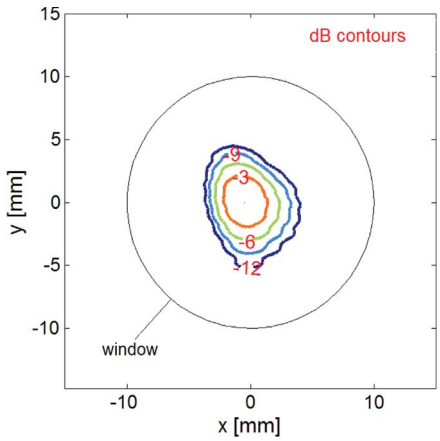

Fig. 4. Simulated electric field of 330-GHz microwave output beam at the focal plane. The beam pattern is displayed in decibel contours. The gyrotron window is shown as reference.

TABLE III
GYROTRON OPERATING PARAMETERS

Operating mode $TE_{m,p,q}$	$TE_{-4,3,q}$
Frequency	328.8 – 330 GHz
Frequency tuning range	1.2 GHz
Output power	2 – 18 W (CW)
Cavity magnetic field B_0	6.0 T
Cyclotron harmonic	Second
Beam voltage $V_{\rm b}$	< 13 kV
Beam current $I_{\rm b}$	190 mA

III. EXPERIMENTAL RESULTS

The 330-GHz second-harmonic gyrotron was characterized in the CW mode with a 19-mm-diameter corrugated waveguide connected to the gyrotron output. The output power of the oscillator was measured using a Scientech laser disk calorimeter, model 36-0401, whereas the frequency was measured using a heterodyne system detailed in [13]. Table III summarizes the main operating parameters of the 330-GHz gyrotron oscillator.

A. Start Oscillation Current

The start oscillation current of the operating mode $TE_{-4,3}$ was evaluated as a function of magnetic field B_0 for a fixed

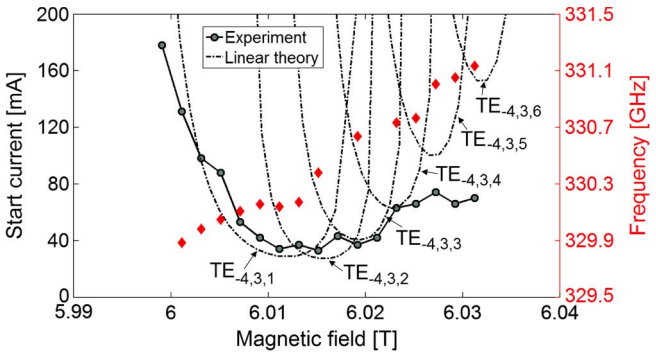

Fig. 5. (Solid line) Measured start oscillation current and (diamonds) measured frequency of the operating mode $TE_{-4,3}$ as a function of magnetic field for beam voltage $V_b = 10.1$ kV and water temperature in the cavity cooling channel $T_{\rm water} = 20$ °C. The theoretical start currents for the first six axial modes $TE_{-4,3,q}$, where $q = 1, 2, 3, 4, 5, 6$, are shown as dash-dotted lines, and they were computed using linear theory (simulation parameters: $r_{\rm cav} = 1.833$ mm, cold-cavity axial field profile, $V_b = 10.1$ kV, $\alpha = 1.8$, and 5% beam perpendicular velocity spread).

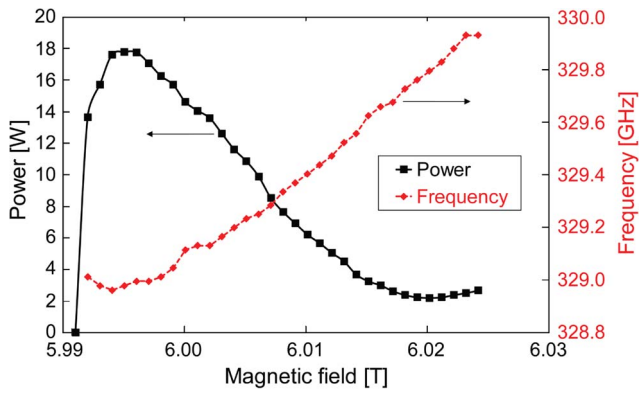

Fig. 6. (Solid line) Power and (dashed line) frequency tuning measurements as a function of magnetic field for beam voltage $V_b = 10.1$ kV, beam current $I_b = 190$ mA, and cavity cooling channel temperature $T_{\rm water} = 9$ °C. The gun coil was swept from $B_{\rm gun} = -3$ mT to $B_{\rm gun} = -5$ mT for the best output power as the magnetic field was increased.

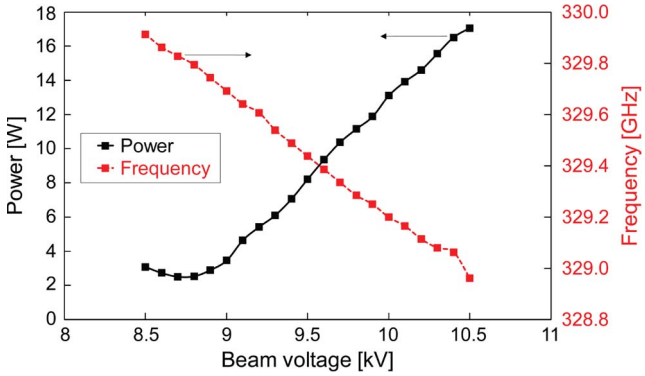

Fig. 7. (Solid line) Power and (dashed line) frequency tuning measurements as a function of beam voltage for magnetic field $B_0 = 6.003$ T, beam current $I_b = 190$ mA, and cavity cooling channel temperature $T_{\rm water} = 9$ °C. The gun coil was swept from $B_{\rm gun} = 1$ mT to $B_{\rm gun} = -25$ mT for the best output power as the beam voltage was decreased.

beam voltage $V_b = 10.1$ kV. The measured start current and the measured frequency at each start current value are displayed in Fig. 5 by a solid line and by diamonds, respectively. The minimum start current was measured to be 33 mA. Fig. 5 also shows the theoretical start currents for the first six axial modes $TE_{-4,3,q}$, where $q = 1$–6. The theoretical start currents were obtained from linear theory for beam parameters $V_b = 10.1$ kV, $\alpha = 1.8$, and 5% electron perpendicular velocity spread. The start current calculations assumed a cavity radius $r_{\rm cav} = 1.833$ mm for the best fit, which is within the experimental error of the value (1.834 mm) obtained from the cavity cold test, as well as the axial electric field profile obtained from the cold-cavity code.

Good agreement is obtained between the measured start current and the prediction from the linear theory, suggesting that high-order axial modes are being observed in the experiment. In addition, the measured frequency range for the start current between 329.88 and 331.13 GHz is in reasonable agreement with the range for high-order axial modes presented in Table I. At each start current point, the excited power was greater than 1.4 W for $B_0 < 6.01$ T and lower than 200 mW for $B_0 > 6.01$ T. Measured frequencies lower than the predicted cutoff of 329.96 GHz from the cold test may be a result of thermal detuning due to the higher excited power at the lower edge of magnetic field values. The neighboring fundamental mode $TE_{5,1}$ is excited for magnetic field values $B_0 > 6.032$ T.

B. Power and Frequency Tuning

The 330-GHz gyrotron has generated 18 W of output power in the second-harmonic mode $TE_{-4,3}$ for a 10.1-kV 190-mA electron beam, which corresponds to an efficiency of 0.93%. A smooth continuous frequency tuning range of 1 GHz has been achieved as a function of magnetic field, as shown in Fig. 6. In the magnetic tuning measurement, the gyrotron output power was optimized by adjusting the subtracting gun coil field from $B_{\rm gun} = -3$ mT to $B_{\rm gun} = -5$ mT as the main magnetic field was increased, resulting in a minimum output power of 2 W throughout the frequency tuning range.

Comparing the magnetic tuning data with the measured start current, one can verify that microwaves are being excited at current values lower than the start current for $B_0 < 6.0$ T. This region corresponds to the hard excitation region, and it is accessible by lowering the magnetic field after first exciting microwaves at a higher magnetic field value. Another difference between Figs. 5 and 6 is a frequency downshift seen in the magnetic tuning measurement for fields below 6.024 T. This frequency shift was not observed in pulsed-mode operation with a duty cycle of 0.004% and a beam current up to 600 mA, and it may be associated to cavity thermal expansion under higher average power operation. At magnetic fields higher than 6.024 T and lower than the threshold to excite the fundamental harmonic mode $TE_{5,1}$, the measured frequency (not shown) is similar to the one observed during the start current measurement.

Due to the dependence of the electron cyclotron frequency on the beam voltage, a continuous tuning range of 1 GHz was also achieved as a function of the beam voltage for a constant magnetic field, as indicated in Fig. 7. As the beam voltage was decreased from the maximum power point, the gun coil field had to be adjusted from $B_{\rm gun} = 1$ mT to $B_{\rm gun} = -25$ mT to optimize the gyrotron power for a beam current $I_b = 190$ mA.

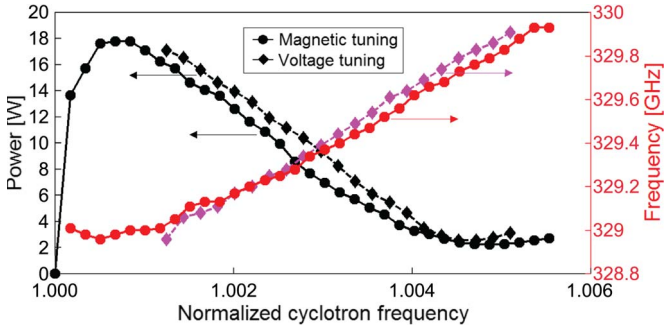

Fig. 8. (Circular marks) Magnetic and (diamond marks) voltage tuning measurements for beam current $I_b = 190$ mA and cavity cooling channel temperature $T_{\text{water}} = 9$ °C. The magnetic and voltage tuning data were taken at $V_b = 10.1$ kV and $B_0 = 6.003$ T, respectively.

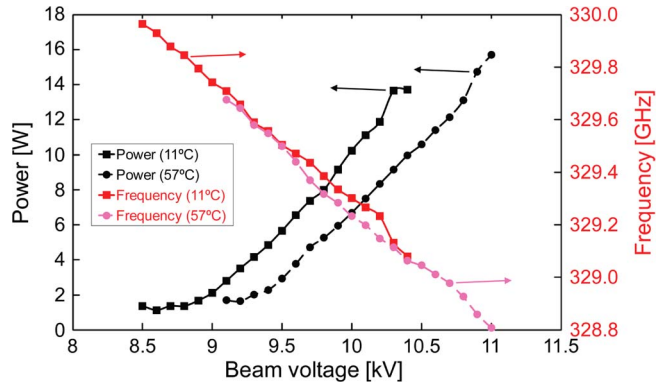

Fig. 9. Voltage tuning measurement for magnetic field $B_0 = 6.003$ T, beam current $I_b = 150$ mA, as well as the cavity cooling channel temperatures (square markers) $T_{\text{water}} = 11$ °C and (circular markers) $T_{\text{water}} = 57$ °C.

The power and the tuning response obtained using voltage tuning are similar to the ones measured for magnetic tuning, as shown in Fig. 8 by plotting the voltage and magnetic tuning results as a function of the normalized electron cyclotron frequency. One advantage of voltage tuning over magnetic tuning is the possibility of sweeping the gyrotron frequency at a faster rate, which may be explored, for instance, in future DNP/NMR experiments.

Another feature evaluated in the 330-GHz gyrotron was frequency tunability via thermal tuning. By increasing the water temperature T_{water} in the cavity cooling channel via a commercial chiller/heater system, the gyrotron cavity will expand, and the beam voltage necessary to keep the same synchronism and efficiency condition has to be increased for a fixed magnetic field. This effect is observed in the measurement shown in Fig. 9, as the power curve shifts to higher voltage values as the water temperature is increased from 11 °C to 57 °C. An additional tuning range of 250 MHz was obtained using thermal tuning. The measured thermal tuning rate of 5 MHz/°C is consistent with the theoretical rate of 5.6 MHz/°C, considering a copper thermal expansion coefficient of 1.7×10^{-5}/°C at 20 °C.

C. CW Long-Term Stable Operation

Stable gyrotron operation over extended periods without interruption is an important requirement to allow long-term signal averaging in DNP/NMR experiments. The stability of the

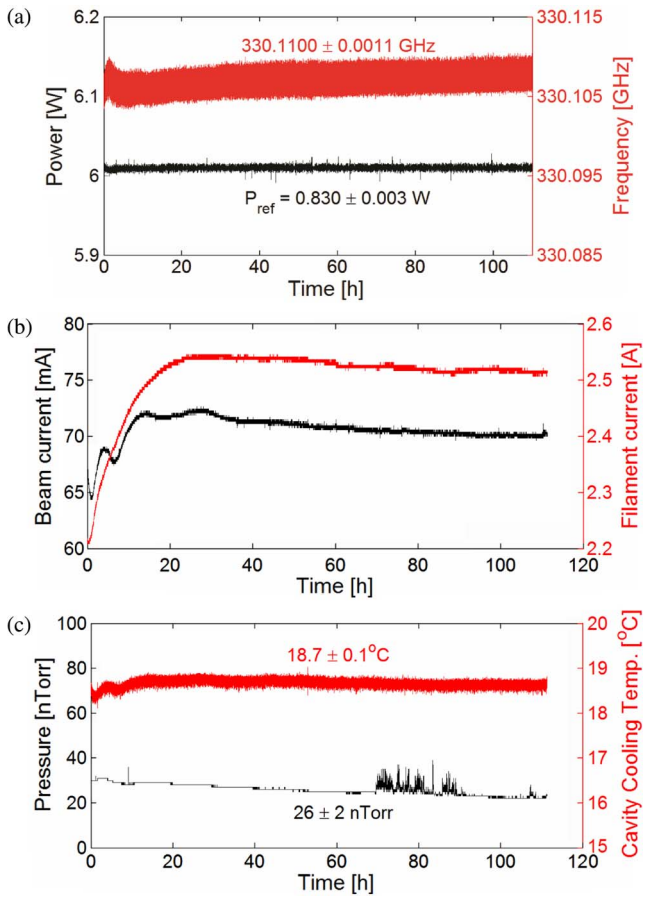

Fig. 10. Monitored variables during the CW long-run stability test of the 330-GHz second-harmonic gyrotron: (a) Output power and frequency, (b) beam and cathode filament currents, and (c) pressure and cavity cooling temperature. During the test, the magnetic field was persistent at $B_0 = 6.006$ T, and the beam voltage was fixed at $V_b = 10.0$ kV.

330-GHz gyrotron was evaluated during a 110-h continuous run test, and the result is shown in Fig. 10. In this test, the output power was kept stable using a proportional, integral, and derivative computerized control system by adjusting the cathode filament current based on the difference between a set point value and the measured output power. During the test, the magnetic field remained in persistent mode at $B_0 = 6.006$ T, whereas the beam voltage and the cavity cooling channel temperature remained constant. The reported stabilities for the magnet in persistent mode, the power supply, and the chiller are 0.02 ppm/h [13], 0.01% over 8 h, and ±0.1 °C, respectively. The gyrotron output power was sampled using a Scientech calorimeter head, model AC2500. During the stability test, the output reference power and frequency were kept stable within ±0.4% (±3 mW) and ±3 ppm (±1.1 MHz), respectively, meeting the requirement for DNP/NMR.

D. Output Beam Pattern

The output microwave beam pattern of the 330-GHz gyrotron was quantitatively evaluated based on images taken using a Spiricon Pyrocam III pyroelectric camera at the end of a corrugated waveguide connected to the gyrotron window. A direct free-space evaluation of the microwave beam in the vicinity of the window was not possible using the pyroelectric camera due

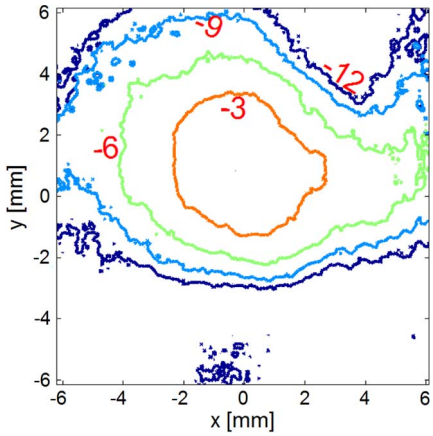

Fig. 11. Gyrotron output microwave beam pattern captured by a pyroelectric camera after the end of the corrugated waveguide. The beam pattern is displayed in decibel contours. Gyrotron parameters: Magnetic field $B_0 = 6.003$ T, beam voltage $V_b = 9.6$ kV, beam current $I_b = 32$ mA, frequency $= 330.17$ GHz, and output power of 0.4 W.

to physical constraints imposed by the utilized superconducting magnet. This required a waveguide to be utilized for the beam pattern measurement, which may have introduced distortions in the measured beam. Due to the camera maximum power limit of 2 W, a picture of the output beam was taken at low power (0.4 W), and it is shown in Fig. 11. The Gaussian-like content associated with the measured pattern was calculated to be 92% with beam radii $w_x = 5.1$ mm and $w_y = 4.0$ mm.

IV. Conclusion

The second-harmonic 330-GHz gyrotron oscillator has generated 18 W of power from a 10.1-kV 190-mA electron beam working in a $TE_{-4,3}$ cylindrical mode, which corresponds to an efficiency of 0.93%. Good agreement has been obtained between the measured start oscillation current and the theoretical start currents calculated from linear theory for successive high-order axial modes $TE_{-4,3,q}$, where $q = 1$–6. In addition, the observed frequency range in the start current measurement is in reasonable agreement with the frequency range expected from numerical calculations. The minimum start oscillation current of the oscillator was measured to be 33 mA. A continuous frequency tuning range of 1.0 GHz with a minimum output power of 2 W was experimentally achieved via magnetic and voltage tuning schemes. While the results from these two tuning schemes basically overlapped, voltage tuning presents as an option to tune the gyrotron frequency at a faster rate, a feature that may be explored by some applications such as DNP/NMR. Thermal tuning has been also implemented and assessed in this tube, yielding an additional tuning range of 250 MHz. Another aspect of the source relevant for the 500-MHz DNP/NMR application for which the gyrotron was designed is the frequency and power stabilities. The gyrotron output power and frequency stabilities have been measured to be $\pm 0.4\%$ and ± 3 ppm, respectively, during a 110-h uninterrupted CW run. The gyrotron output microwave beam pattern has been also measured using a pyroelectric camera, and it has a Gaussian-like mode content of 92% with an ellipticity of 28%, indicating a suitable operation of the manufactured mode converter.

Acknowledgment

The authors gratefully acknowledge the technical assistance from Mr. I. Mastovsky.

References

[1] M. K. A. Thumm, "Recent developments on high-power gyrotrons—Introduction to this special issue," *J. Infrared Millim. Terahz. Waves*, vol. 32, no. 3, pp. 241–252, Mar. 2011.

[2] V. L. Bratman, M. Y. Glyavin, Y. K. Kalynov, A. G. Litvak, A. G. Luchinin, A. V. Savilov, and V. E. Zapevalov, "Terahertz gyrotrons at IAP RAS: Status and new designs," *J. Infrared Millim. Terahz. Waves*, vol. 32, no. 3, pp. 371–379, Mar. 2011.

[3] S. Spira-Hakkarainen, K. E. Kreischer, and R. J. Temkin, "Submillimeter-wave harmonic gyrotron experiment," *IEEE Trans. Plasma Sci.*, vol. 18, no. 3, pp. 334–342, Jun. 1990.

[4] K. L. Felch, B. G. Danly, H. R. Jory, K. E. Kreischer, W. Lawson, B. Levush, and R. J. Temkin, "Characteristics and applications of fast-wave gyrodevices," *Proc. IEEE*, vol. 87, no. 5, pp. 752–781, May 1999.

[5] H. Bindslev, J. A. Hoekzema, J. Egedal, J. A. Fessey, T. P. Hughes, and J. S. Machuzak, "Fast-ion velocity distributions in JET measured by collective Thomson scattering," *Phys. Rev. Lett.*, vol. 83, no. 16, pp. 3206–3209, Oct. 1999.

[6] L. R. Becerra, G. J. Gerfen, R. J. Temkin, D. J. Singel, and R. G. Griffin, "Dynamic nuclear polarization with a cyclotron resonance maser at 5 T," *Phys. Rev. Lett.*, vol. 71, no. 21, pp. 3561–3564, Nov. 1993.

[7] K. Felch, M. Blank, P. Borchard, P. Cahalan, S. Cauffman, and H. Jory, "Recent test results on a 95 GHz, 2 MW gyrotron," in *Proc. 33rd Int. Conf. Infrared, Millim. THz Waves*, Pasadena, CA, Sep. 2008, pp. 1–2.

[8] V. S. Bajaj, M. K. Hornstein, K. E. Kreischer, J. R. Sirigiri, P. P. Woskov, M. L. Mak-Jurkauskas, J. Herzfeld, R. J. Temkin, and R. G. Griffin, "250 GHz CW gyrotron oscillator for dynamic nuclear polarization in biological solid state NMR," *J. Magn. Reson.*, vol. 189, no. 2, pp. 251–279, Dec. 2007.

[9] Y. V. Zasypkin, "Electronic frequency tuning in gyrotrons," *Sov. J. Commun. Technol. Electron.*, vol. 33, no. 5, pp. 7–13, May 1988.

[10] M. K. Hornstein, V. S. Bajaj, R. G. Griffin, K. E. Kreischer, I. Mastovsky, M. A. Shapiro, J. R. Sirigiri, and R. J. Temkin, "Second harmonic operation at 460 GHz and broadband continuous frequency tuning of a gyrotron oscillator," *IEEE Trans. Electron Devices*, vol. 52, no. 5, pp. 798–807, May 2005.

[11] M. K. Hornstein, V. S. Bajaj, R. G. Griffin, and R. J. Temkin, "Efficient low-voltage operation of a CW gyrotron oscillator at 233 GHz," *IEEE Trans. Plasma Sci.*, vol. 35, no. 1, pp. 27–30, Feb. 2007.

[12] A. C. Torrezan, S.-T. Han, M. A. Shapiro, J. R. Sirigiri, and R. J. Temkin, "CW operation of a tunable 330/460 GHz gyrotron for enhanced nuclear magnetic resonance," in *Proc. 33rd Int. Conf. Infrared, Millim. THz Waves*, Pasadena, CA, Sep. 2008, pp. 1–2.

[13] A. C. Torrezan, S.-T. Han, I. Mastovsky, M. A. Shapiro, J. R. Sirigiri, R. J. Temkin, A. B. Barnes, and R. G. Griffin, "Continuous-wave operation of a frequency-tunable 460-GHz second-harmonic gyrotron for enhanced nuclear magnetic resonance," *IEEE Trans. Plasma Sci.*, vol. 38, no. 6, pp. 1150–1159, Jun. 2010.

[14] T. H. Chang, T. Idehara, I. Ogawa, L. Agusu, and S. Kobayashi, "Frequency tunable gyrotron using backward-wave components," *J. Appl. Phys.*, vol. 105, no. 6, p. 063 304, Mar. 2009.

[15] T. Idehara, K. Kosuga, L. Agusu, R. Ikeda, I. Ogawa, T. Saito, Y. Matsuki, K. Ueda, and T. Fujiwara, "Continuously frequency tunable high power sub-THz radiation source—Gyrotron FU CW VI for 600 MHz DNP-NMR spectroscopy," *J. Infrared Millim. Terahz. Waves*, vol. 31, no. 7, pp. 775–790, Jul. 2010.

[16] A. C. Torrezan, M. A. Shapiro, J. R. Sirigiri, and R. J. Temkin, "A tunable continuous-wave 330 GHz gyrotron for enhanced nuclear magnetic resonance," in *Proc. IEEE 36th Int. Conf. Plasma Sci.*, San Diego, CA, Jun. 2009, p. 1.

[17] I. I. Antakov, S. N. Vlasov, V. A. Gintsburg, L. I. Zagryadskaya, and L. V. Nikolaev, "CRM-oscillators with mechanical tuning of frequency," *Elektron. Tekhn.*, ser. I, Elektron. SVCh, no. 8, pp. 20–25, 1975.

[18] G. F. Brand, Z. Chen, N. G. Douglas, M. Gross, J. Y. L. Ma, and L. C. Robinson, "A tunable millimetre-submillimetre gyrotron," *Int. J. Electron.*, vol. 57, no. 6, pp. 863–870, 1984.

[19] H. Shoyama, K. Sakamoto, K. Hayashi, A. Kasugai, M. Tsuneoka, K. Takahashi, Y. Ikeda, T. Kariya, Y. Mitsunaka, and T. Imai, "High-efficiency oscillation of 170 GHz high-power gyrotron at $TE_{31,8}$ mode

using depressed collector," *Jpn. J. Appl. Phys.*, vol. 40, no. 8B, pp. L906–L908, Aug. 2001.
[20] W. B. Herrmannsfeldt, "EGUN—An electron optics and gun design program," SLAC, Stanford, CA, Tech. Rep. SLAC-331 UC-28, Oct. 1988.
[21] A. W. Fliflet and M. E. Read, "Use of weakly irregular waveguide theory to calculate eigenfrequencies, Q values, and RF field functions for gyrotron oscillators," *Int. J. Electron.*, vol. 51, no. 4, pp. 475–484, 1981.
[22] M. Yeddulla, G. S. Nusinovich, and T. M. Antonsen, Jr., "Start currents in an overmoded gyrotron," *Phys. Plasmas*, vol. 10, no. 11, pp. 4513–4520, Nov. 2003.
[23] J. M. Neilson and R. Bunger, "Surface integral equation analysis of quasi-optical launcher," *IEEE Trans. Plasma Sci.*, vol. 30, no. 3, pp. 794–799, Jun. 2002.

Antonio C. Torrezan (S'04–M'10) received the B.S. and M.S. degrees in electrical engineering from the State University of Campinas (UNICAMP), Campinas, Brazil, in 2004 and 2005, respectively, and the Ph.D. degree in electrical engineering and computer science from Massachusetts Institute of Technology (MIT), Cambridge, in 2010.

From 2003 to 2005, he was associated with the Brazilian Synchrotron Light Laboratory (LNLS), Campinas, Brazil, where his research was focused on the development of an X-band electron paramagnetic resonance spectrometer for samples with a small number of spins. In 2004, he worked as an Intern with the Brazilian Aeronautics Co. (Embraer), São José dos Campos, Brazil, in the area of control systems. From 2005 to 2010, he worked as a Research Assistant with the Plasma Science and Fusion Center, MIT, developing continuously tunable continuous-wave terahertz gyrotron oscillators for dynamic nuclear polarization in nuclear magnetic resonance. Since 2010, he has been a Postdoctoral Research Associate with the Hewlett-Packard Co., Palo Alto, CA, working on the next generation of nonvolatile resistive memory. His research interests include high-speed circuits, microwave and terahertz technologies, and vacuum electron devices such as gyrotrons.

Michael A. Shapiro received the Ph.D. degree in radio physics from the University of Gorky, Gorky, Russia in 1990.

Since 1995, he has been with the Plasma Science and Fusion Center, Massachusetts Institute of Technology, Cambridge, where he is currently the Head of the Gyrotron Research Group. His research interests include vacuum microwave electron devices, high-power gyrotrons, dynamic nuclearpolarization spectroscopy, high-gradient linear accelerators, quasi-optical millimeter-wave components, and photonic band-gap structures and metamaterials.

Jagadishwar R. Sirigiri (S'98–M'03) received the B. Tech. degree in electronics engineering from the Indian Institute of Technology, Varanasi, India, in 1996 and the S.M. and Ph.D. degrees in electrical engineering and computer science from Massachusetts Institute of Technology (MIT), Cambridge, in 2000 and 2003, respectively.

He has over 15 years of experience in experimental and theoretical aspects of microwave engineering, vacuum electron devices, and terahertz technology. During his undergraduate work with the Indian Institute of Technology, Varanasi, India, he worked on the theory of gyrotrons and traveling-wave tubes (TWTs) and developed an automated system for the characterization of dispersion and interaction impedance of helical slow-wave structures. From 1996 to 1998, he was a Senior Hardware Engineer with Wipro Infotech, India, where he was involved in the development of multimedia products, including hardware-based videoconferencing solutions. He was a Research Scientist with MIT, where he was the Leader of the experimental program on high-power microwave and terahertz source development including gyrotrons and other types of sources for application in dynamic nuclear polarization (DNP) in nuclear magnetic resonance (NMR), electron paramagnetic resonance (EPR), fusion plasma heating, and radar. He is the founder of Bridge12 Technologies Inc., Cambridge, MA, which develops terahertz systems for applications in science, medicine, security, and in defense. His research resulted in several accomplishments including the experimental demonstration of efficiency exceeding 50% in a megawatt-class gyrotron for plasma heating application, the theoretical and experimental research on after-cavity interaction in gyrotrons and its effect on efficiency, the theoretical and experimental work on the low-frequency oscillations in megawatt gyrotron oscillators, the development of tunable continuous-wave gyrotron oscillators in the millimeter wave and terahertz range and their successful application in high-field DNP-NMR spectroscopy, and the development of high-power high-frequency gyrotron TWT amplifiers at 140 and 250 GHz for applications in radar and EPR and overmoded TWT amplifiers. He demonstrated the first vacuum electron device with a photonic-band-gap structure to suppress mode competition while operating in a higher order mode.

Dr. Sirigiri is a member of the American Physical Society, the Union of Concerned Scientists, and Sigma Xi. He served as a Guest Editor of the 12th Special Issue on High-Power Microwave Generation of the IEEE TRANSACTIONS ON PLASMA SCIENCES in 2008.

Richard J. Temkin (M'87–SM'92–F'94) received the B.A. degree in physics from Harvard College, Cambridge, MA, and the Ph.D. degree in physics from Massachusetts Institute of Technology (MIT), Cambridge.

From 1971 to 1974, he was a Postdoctoral Research Fellow with the Division of Engineering and Applied Physics, Harvard University. Since 1974, he has been with MIT, first with the Francis Bitter National Magnet Laboratory and later with the Plasma Science and Fusion Center (PSFC) and the Department of Physics. He is currently a Senior Scientist with the Department of Physics, the Associate Director of the PSFC, and the Head of the Waves and Beams Division, PSFC. His research interests include novel vacuum electron devices such as the gyrotron and the free-electron laser, advanced high-gradient electron accelerators, overmoded waveguides and antennas at millimeter/terahertz wavelengths, high-power microwave sources and their applications, plasma heating, and dynamic nuclear polarization/nuclear magnetic resonance. He has authored or coauthored over 200 published journal articles and book chapters and has been the Editor of six books and conference proceedings.

Dr. Temkin is a Fellow of the American Physical Society and The Institute of Physics, London, U.K. He was the recipient of the Kenneth J. Button Prize and Medal of The Institute of Physics and the Robert L. Woods Award of the Department of Defense for Excellence in Vacuum Electronics research.

Robert G. Griffin, photograph and biography not available at the time of publication.